

# Photonic Radar for 3D Imaging: From Millimeter to Terahertz Waves

Li Yi , Member, IEEE, Yihan Li , Member, IEEE, and Tadao Nagatsuma , Fellow, IEEE

(Invited Paper)

**Abstract**—With the development of 5G and other technologies, radar imaging techniques in high-frequency bands up to the terahertz (THz) range have attracted considerable attention. In particular, the photonic radar technique benefits from the unique advantages of optical devices, including an ultrawide and flexible bandwidth of more than 100 GHz, leading to submm-order range resolution, reduced phase noise, and flexible optical links. This article reviews recent progress in photonic radar systems from the millimeter wave to THz bands, including the hardware components, imaging technology, and radar imaging applications, and discusses the potential high-resolution imaging techniques enabled by photonic radar systems.

**Index Terms**—Photomixing, photonic mixer, photonic radar, synthetic aperture radar, terahertz imaging.

## I. INTRODUCTION

**I**MAGING techniques using electromagnetic (EM) waves in microwave bands have been studied for decades by electronics and photonics researchers due to their unique penetration abilities [1], [2], [3]. Compared with the established imaging instruments and techniques, novel imaging systems in higher frequency bands, such as the millimeter wave (MMW, 30-100 GHz), sub-terahertz (sub-THz, 0.1-0.3 THz), and THz (0.3 THz-10 THz) bands, have attracted significant attention, as these frequencies lead to considerably improved spatial resolution due to their higher frequencies and wider bandwidths. For example, THz band imaging systems have demonstrated submillimeter-level resolution and transparency for electrical insulators such as paper, glass, and polymers [2], [3], [4], [5]. More importantly, these frequency bands can be used for wireless communication and industrial applications since they do not harm the human body. Because of these advantages, these inspection techniques

Manuscript received 18 January 2023; revised 26 June 2023 and 19 July 2023; accepted 21 July 2023. Date of publication 26 July 2023; date of current version 9 August 2023. This work was supported in part by JST, ACT-X under Grant JPMJAX22K2, in part by the ROHM Company, Ltd., in part by the Commissioned Research of the National Institute of Information and Communications Technology, Japan, under Grant 02801, and in part by the KAKENHI under Grant 20H00253. (Li Yi and Yihan Li contributed equally to this work.) (Corresponding author: Li Yi.)

Li Yi and Tadao Nagatsuma are with the Graduate School of Engineering Science, Osaka University, Toyonaka, Osaka 560-8531, Japan (e-mail: yi@ee.es.osaka-u.ac.jp; nagatsuma@ee.es.osaka-u.ac.jp).

Yihan Li is with the School of Integrated Circuit Science and Engineering, Beihang University, Beijing 100191, China (e-mail: yihanli@buaa.edu.cn).

Color versions of one or more figures in this article are available at <https://doi.org/10.1109/JSTQE.2023.3298933>.

Digital Object Identifier 10.1109/JSTQE.2023.3298933

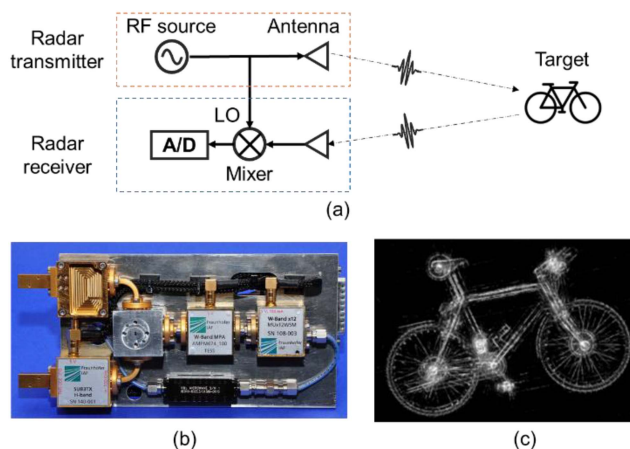


Fig. 1. Concept and example of an electronic radar imaging system: (a) Simplified radar schematic diagram; (b) 300-GHz band radar imaging system. A spatial resolution of  $\sim 4$  mm was achieved using a total bandwidth of  $\sim 40$  GHz. (c) Imaging result obtained with the SAR method. A bicycle  $\sim 140$  m away can be clearly imaged, including the details of the wire wheels. Reprinted with permission from [12].

can be particularly useful in applications such as medicine [6], [7], nondestructive testing (NDT) [8], [9], security [10], and remote sensing [11].

Compared with 2D imaging that obtains the 2D mapping through the obstacles, the 3D information is highly desirable since the shape, depth, and distribution of imaging targets occluded by obstacles can be detected. In this case, the radio detection and ranging (Radar) technology is commonly applied to obtain the range information of the obstacles and targets for 3D imaging. In general, a radar system transmits the radar waveforms generated by voltage-controlled oscillators (VCOs) and receives the reflected signals with a mixer to measure the time delay to the targets. Then, the time delays at different positions are utilized to create 2D or 3D images using synthetic aperture radar (SAR) algorithms, as shown in Fig. 1. Electronic radar systems with frequency multiplexing techniques have gradually obtained higher spatial resolution over the past decades. One of the most representative works is MIRANDA-300, an ultrawideband radar imaging system in the 300-GHz band [12]. Notably, although several years have passed since the publication of this work in 2014, reproducing the results remains quite challenging, as the advanced high-frequency radio frequency (RF) components

utilized in the system, such as the mixers and preamplifiers, are sophisticated pieces of equipment.

Furthermore, radar signals up to  $\sim 1$  THz with more than 100 GHz bandwidth can be generated and detected using high-end electronic instruments, such as vector network analyzers (VNAs), based on which a series of 3D imaging demonstrations have been reported ranging from the MMW band to the THz band [13], [14], [15], [16]. These refined techniques offer superior bandwidth and mW-order output power. However, in addition to the increasingly complicated structure and thus increased cost at higher frequency bands, the imaging speed, which is limited by the switching speed of frequencies in electronic signal generators with large bandwidths [12], [17], and phase noise, which deteriorates due to frequency multiplexing [18], [19], are fundamental bottlenecks for electronic devices.

In addition to the multistage frequency multiplexing technique, high-frequency diode oscillators such as impact-ionization avalanche transit time (IMPATT) diodes [20], Gunn diodes [21], [22], and resonant tunneling diodes (RTDs) [23], [24], [25] have been rapidly developed in recent years, with numerous imaging applications reported. Although an oscillating frequency up to  $\sim 2$  THz has been reported using an RTD [26], the insufficiently tunable bandwidth and unstable tunability must be addressed to enable high-resolution 3D imaging [25], [27].

Meanwhile, optics itself has a long history of imaging, but mostly in parallel with radio frequency (RF) counterparts until the prevalence of electro-optical and optoelectronic components. To overcome the limitations mentioned above of purely electronic approaches, extensive study has been devoted to photonics-assisted methods for 3D imaging and radar applications from the MMW band to the THz band [4], [5], [19], [28], [29], [30], [31], [32], [33], [34], [35], [36], [37], [38], [39], [40], [41], [42], [43], [44], [45], [46], [47], [48], [49], [50], [51]. The frequency and bandwidth requirements for high-resolution imaging in the MMW and THz bands that are too demanding for electronics become fractional in the optical region, where the spectral abundance can be transferred to other dimensions for reconfigurability. Moreover, the down-conversion nature of photonic RF generation methods addresses the phase noise scaling issue of electrical up-conversion schemes, enabling high spectral purity in the higher frequency bands. These intrinsic advantages of photonics-based waveform manipulation techniques have been observed in both radar and wireless communication applications. As these two fields share essentially the same photonic structure and key components, advantages of the photonic techniques such as wide and flexible bandwidths, tunable phase shifts, and reduced phase noise are experimentally demonstrated [45], [52], [53]. Analogically, photonic-based radar technologies offer an enhanced spatial resolution, increased acquisition speed, and small size, weight, and power (SWaP) for target identification. These techniques may promote new ideas for the next generation of practical THz 3D imaging systems.

This article highlights some recent progress and advantages of photonic techniques in 3D imaging and radar applications in the MMW to THz bands. The basics of the photonic radar system, including the radar waveform, imaging techniques, and hardware components, are summarized in Section II. Section III

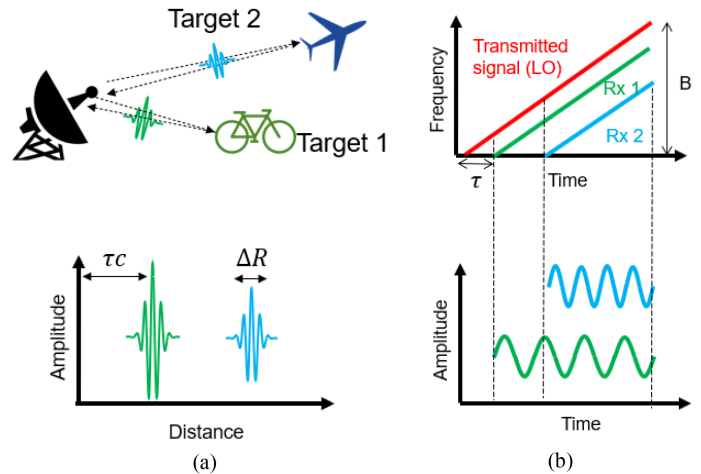


Fig. 2. Concepts of pulse and CW radar systems: (a) Concept of a pulse radar system: a pulse signal with a pulse width proportional to the range resolution  $\Delta R$  is reflected at the imaging targets, and the travel time  $\tau$  can be converted into a distance based on the speed of light  $c$ . (b) Corresponding FMCW radar configuration. The upper figure indicates the transmitted signal and two reflected signals ( $R_x$ ) in the frequency-time domain, while the lower figure indicates the F signal obtained by mixing  $T_x$  and  $R_x$ . A similar result to that of the pulse radar system can be obtained using FFTs.

presents the advantages of photonic radar systems by introducing the related applications and comparing their features. Imaging scenarios in different ranges are introduced for various operating frequencies in the MMW to THz bands. The prospects of related techniques, which have not yet been installed in existing photonic radar systems, are discussed in Section IV. Finally, the conclusions are presented in Section V. Despite the authors best efforts, all the exciting research that has been reported worldwide could not be covered in this article. The topics discussed here should be understood as a representative cross-section of recent global trends.

## II. PHOTONIC RADAR SYSTEMS FROM MMW TO THZ BANDS

### A. Fundamentals of Radar Imaging Systems: Pulse vs. Continuous Wave (CW)

Radar techniques were developed to estimate target distance, angle, and velocity information. The basic concept of radar techniques is to measure the time delay between the transmitted and received EM pulses, which can then be converted to range information based on the known propagation velocity of the EM wave, as shown in Fig. 2(a). Additionally, radar systems can be categorized based on the pulse generation method, namely, pulse radar and continuous-wave (CW) radar systems. The features of both systems are summarized in Table I with details introduced below.

A shorter pulse can improve the range resolution but requires a wider bandwidth, which increase the complexity and the cost of the system. Depending on the specific scenario, radar systems can be configured to different frequency bands to obtain the imaging distance, spatial resolution, and penetration ability required by the given application. For example, a microwave-band ground penetrating radar (GPR) system operating at  $\sim 500$

TABLE I  
 BRIEF COMPARISON OF PULSE AND CW RADAR TECHNIQUES

	ADVANTAGES	LIMITATIONS
<b>PULSE RADAR</b>	Simpler system <sup>1</sup> ; up to a few THz <sup>2</sup> .	Energy limited by pulse duration; up to a few GHz <sup>3</sup> .
<b>CW RADAR</b>	Enhanced SNR; adjustable frequency bands.	Challenging for huge bandwidth of >100 GHz; complicated signal processing.

<sup>1</sup> below MMW bands; <sup>2</sup> photonics-based; <sup>3</sup> electronics-based.

MHz can penetrate a few meters into the subsurface with a spatial resolution of cm-order [1], [54]. In addition, a THz pulse imaging system can obtain  $\mu\text{m}$ -order resolution but can only penetrate thin layers of a few millimeters [5], [34]. Both systems directly generate short pulses and detect the time delays of echo signals, thus categorized as pulse radar systems [55]. The key limitation of pulse radar systems is the pulse generation technique, which can reach up to the ps-order with electronic devices [1]. While the THz pulses emitted by femtosecond lasers using photonic technologies can provide ultra-high resolution, the insufficient energy of the short pulse limits its imaging distance. This approach is commonly used in THz time-domain spectroscopy (THz-TDS) systems, which can provide both 3D imaging information and material characterization information [5]. Notably, MMW-band pulse signals can be generated using photonic technology [56]; however, the advantages of photonic systems over electronic systems in this band have not been illustrated.

Compared with pulse systems, in which energy is released in periodic bursts, CW radar systems constantly emit energy into free space. Coherent detection, which is usually realized with a mixer, is then applied to determine the phase delay between the transmitted and received signals. CW radar systems with a single frequency can estimate the velocity of a target by examining the Doppler frequency shift [55]. To obtain the range information, signals with multiple frequencies, such as stepped-frequency continuous waves (SFCWs) or frequency-modulated continuous waves (FMCWs), are required [55]. In the case of the FMCW technique shown in Fig. 2(b), a chirp signal with a bandwidth of  $B$  is emitted, and the received echo is mixed with the local oscillator (LO) signal, generating an intermediate frequency (IF) known as the beat signal. Each target distance corresponds to one unique frequency in the IF signal, which can be determined by applying a fast Fourier transform (FFT). The maximum achievable range resolution  $\Delta R$  of the FMCW system is generally expressed as:

$$\Delta R = \frac{c}{2B} \quad (1)$$

where  $c$  is the speed of the EM wave and  $B$  is the bandwidth of the chirp signal. The above analysis indicates that a broad bandwidth and an accurate mixing process are critical for the FMCW technique to obtain a high resolution. These characteristics also apply to other similar technologies, such as the SFCW radar

 TABLE II  
 COMPARISON OF SAR AND QUASI-OPTICAL IMAGING

	ADVANTAGES	LIMITATIONS
<b>SAR</b>	Flexible 3D imaging region; simple optical alignment; sparse sampling/array is possible	Complicated signal processing; high output power is required.
<b>QUASI-OPTICAL</b>	Less signal processing; simple propagation path; enhanced SNR by focusing.	Fixed imaging distances; dense sampling/array is required; bulky system & complex alignment

and optical coherence tomography (OCT) systems introduced in [14], [48], [57].

In this case, CW radar systems use synthesized broadband waveforms with considerably stretched temporal profiles. As a result, the instantaneous power emitted by the radar transmitter can effectively be regarded as continuous. Moreover, radar theory suggests that these radars can achieve the exact range resolution if the continuous waveform occupies the same bandwidth as its pulse counterpart. However, the considerable variation in the transmitted energy makes a large difference. As almost all radar system components are restricted in terms of instantaneous power, the energy radiated by a pulse radar system is significantly less than that radiated by a CW system, making these systems more vulnerable in high propagation loss scenarios [1].

Due to the technical difficulties in generating ps-order pulses and the long imaging distance requirements, CW radar techniques are crucial in the MMW and sub-THz bands, which are the prime frequency bands considered in this article. Thus, CW techniques are addressed in the following sections. Notably, the combination of wireless communication and radar systems has become an increasingly popular topic. In these systems, other modulation techniques, including orthogonal frequency division multiplexing (OFDM), multifrequency continuous wave (MFCW) approaches, and quadrature phase-shift keying (QPSK), are introduced into radar applications to implement wireless communication [58], [59]. However, regardless of the applied methods, the overall goal is to obtain a synthesized pulse signal to determine the range information, as shown in Fig. 2.

### B. Radar Imaging Techniques: Synthetic Aperture Radar (SAR) and Quasi-Optical Imaging

Radar signals can indicate the time delays of targets; however, a focused beam is necessary to obtain the desired spatial resolution in imaging applications, as shown in Fig. 3. Signal processing methods using the synthetic aperture radar (SAR) technique and quasi-optical beam focusing can be used to obtain high-resolution images. However, the applicable scenarios and the frequency bands are different, as briefly summarized in Table II.

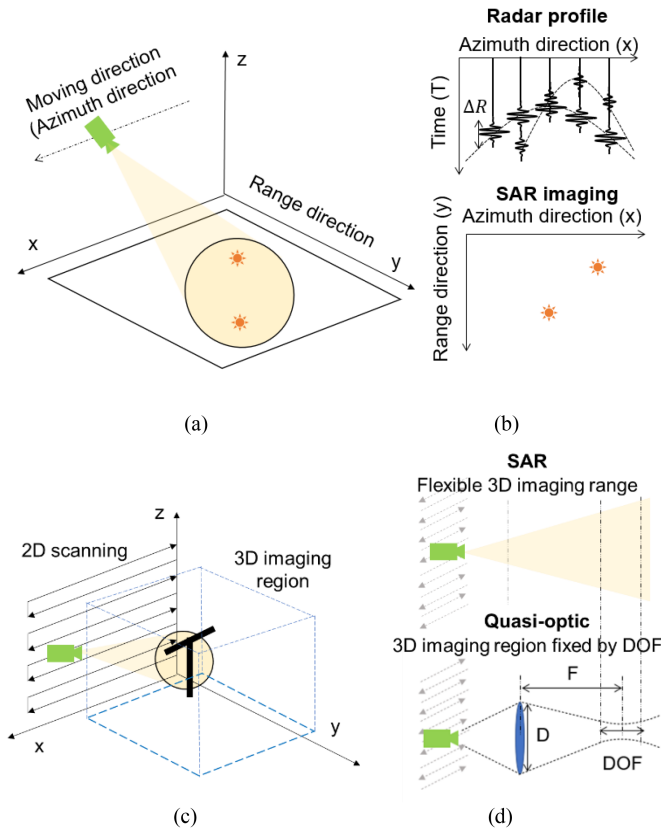


Fig. 3. Features of the SAR and quasi-optical imaging techniques: (a) Side-looking SAR configuration for 2D imaging; (b) example of SAR processing of two scatterers; (c) 3D SAR imaging configuration; (d) comparison of SAR configuration and quasi-optical beam focusing.

Due to the wide radiation pattern below the MMW band, the use of a lens to focus the EM waves, as in a camera, is unrealistic. Instead of using a focusing lens to obtain the desired spatial resolution, the SAR imaging technique is widely used for microwave imaging [49], [55], [60], [61]. The SAR technique is commonly applied in airborne SAR systems, also referred to as side-looking SAR, because of the inclined observation angle with respect to the imaging plane, as shown in Fig. 3(a). This configuration aims at obtaining large-scale 2D images of far-field targets. The time delay information of a target is sampled at different positions along a survey line, and the radar profile is converted into a 2D image using SAR algorithms, as shown in Fig. 3(b). The spatial resolution of the SAR image is defined by the range and azimuth resolution, which correspond to the resolutions in the  $x$ - and  $y$ -directions, respectively. The inclined observation angle is used to convert the radar range resolution, expressed in (1), to the range resolution ( $y$ -direction). In theory, the azimuth resolution can be estimated based on half the antenna length, which is inversely proportional to the bandwidth [61].

Alternatively, 3D images of specific regions can be acquired with 2D spatial sampling methods instead of 1D survey lines, as shown in Fig. 3(c). The primary aim of this 3D SAR configuration is to obtain detailed target information at different depths. This SAR configuration is mainly applied in GPR, through-wall radar, and NDT applications. Notably, 3D SAR techniques also

include migration and tomography techniques in seismic exploration and ultrasonic imaging applications [60], [62]. The range resolution is crucial to distinguish targets with complicated layered structures. In this case, the incident angle of the antenna is perpendicular to the target plane, thereby maximizing the range resolution. In other words, the side-looking SAR configuration projects the 3D depth information to the range direction on the ground surface with an inclined observation angle. The maximum spatial resolution of the 3D SAR configuration can also be estimated based on the half bandwidth. Notably, spatial resolution is affected by other factors, such as limited observation angles, the SAR algorithm, and signal-to-noise ratio (SNR). More details can be found in [55], [60]. The most significant feature of the 3D SAR imaging method is that high-resolution images can be obtained at any distance using bandwidth information instead of focusing lenses. However, a key limitation of SAR imaging methods is that the algorithms require substantial calculations, especially for 3D imaging scenarios.

Since the antenna radiation pattern is narrower above the sub-THz band, quasi-optical imaging systems have been widely applied in many THz imaging systems [4], [63], [64], [65]. The spatial resolution  $\Delta x$  obtained with a focusing lens is limited by the diffraction limit, which can be expressed as:

$$\Delta x \approx 0.61 \frac{\lambda F}{D}, \quad (2)$$

where  $F$  is the focal length,  $\lambda$  is the wavelength, and  $D$  is the diameter of the lens. SAR methods and quasi-optical systems both obtain spatial resolutions close to the half wavelength. However, quasi-optical systems perform better in terms of experimental results since these systems are less affected by unnecessary reflections and the imaging algorithm than SAR configurations. Moreover, since the energy is directly focused on the target, quasi-optical systems also obtain better SNRs than SAR configurations.

The fixed depth of focus (DOF) is a bottleneck for imaging targets at different distances within a 3D space. This issue limits the performance of existing systems when complete 3D information is needed, as shown in Fig. 3(d). However, when the imaging range of interest is small, such as estimating the  $\mu\text{m}$ -order thickness of a coating material in the THz band, a cm-order DOF is sufficient. In addition, an advanced lens design can further extend the DOF while maintaining high spatial resolution [66], [67].

Note that both techniques require spatial sampling that satisfies the Nyquist sampling criterion, which indicates that the spatial sampling interval should be less than half the wavelength. Due to the dense spatial sampling requirements, imaging applications in higher frequency bands are typically time-consuming. Although the SAR technique and compressed sensing can potentially reduce the spatial sampling interval, an ultimate array technique applicable across the MMW to THz bands should be developed. A brief review and perspective of the array and integration technique is presented in Section IV; however, the following sections do not focus on the array technique since it is not the main scope of this article.

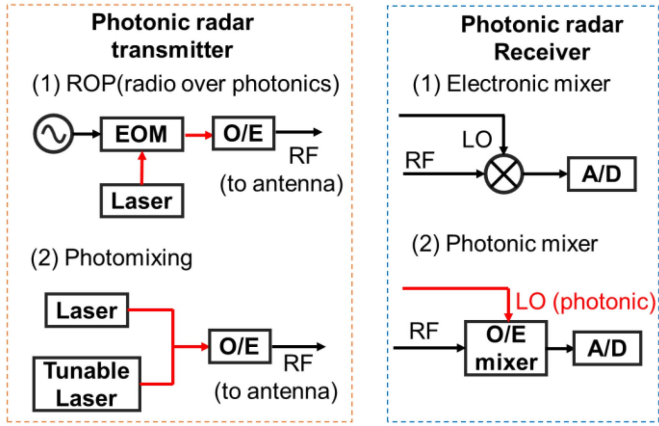


Fig. 4. Concept and categories of electronic and photonic radar systems; the red lines indicate optical fibers, while the black lines indicate coaxial cables.

TABLE III  
RECENT RADAR IMAGING TECHNIQUES ENABLED WITH PHOTONIC TECHNOLOGY

Radar receiver	Radar transmitter	MMW (30-100 GHz)	Sub-THz and THz (0.1-10 THz)
Electronic mixer	ROP	[28]	[29]
	Photomixing	[19], [46], [47]	[4], [48]–[51]
Photonic mixer	ROP	[39]–[45]	N/A
	Photomixing	[35]–[38], [45]	[5], [30]–[34]

### C. Photonic Radar Components

The core techniques of the radar system shown in Fig. 1(a) are radar waveform generation with radar transmitters and coherent detection of LO and RF signals with radar receivers. An ideal photonic radar system is a radar system in which all electronic devices are replaced with their photonic counterparts. However, as photonic radar systems are still at the early stages of development, it is not practical to use photonic devices across all frequency bands. Thus, radar systems partially enabled by photonic devices are also considered photonic radar systems.

The existing photonic radar systems can be categorized based on different combinations of photonic radar transmitter and receiver techniques, as shown in Fig. 4. Furthermore, existing photonic radar imaging systems utilizing these techniques are summarized in Table III. This table provides a general overview linking the different devices and applicable frequency bands.

The signal generation methods used by photonic radar transmitters can be divided into optically carried RF signal synthesis and optical-to-electrical conversion (O/E) techniques. Depending on whether a wideband RF source is needed, optically carried RF signal synthesis methods can be further categorized into radio over photonics (ROP) and photomixing techniques. In contrast, photonic radar receivers are categorized based on

whether electronic or photonic mixing techniques are applied. The features of the two optically carried RF signal synthesis technologies and the O/E devices at different frequencies are detailed in 1), while the features of the corresponding electronic and photonic mixers (O/E mixers) are presented in 2). In addition to the hardware components discussed below, the advantages of photonic radar systems and system applications are described in Section III.

1) *Photonic Radar Transmitters*: As shown in Fig. 4, the ROP method directly modulates a wideband RF signal, which is a chirp signal for the FMCW system, into the optical domain through electro-optical modulation (EOM) [28]. The bandwidth and center frequency of the input can be improved by photonic techniques such as high-order sideband filtering [29]. These techniques also lead to a low phase noise by mixing the radar signal in the optical domain [39], [45]. Most importantly, as the chirping of the output RF signal originates from the electronic input, the instantaneous frequency of the generated waveform is completely controllable and can be fully referenced. As a result, this type of approach is compatible with other electronic devices used in radar systems. However, the low-efficiency nonlinear process of EOM often limits the spectral magnification to only single digits. As a result, the frequency and bandwidth of the output waveform are still restricted by the electronic synthesizer that provides the input signal. Thus, this method cannot be applied in ultrafine resolution imaging scenarios that require high frequencies and/or large bandwidths [45].

Another group of techniques that addresses these frequency and bandwidth restrictions is the heterodyning of two optical tones, also referred to as photomixing [52], [53]. This method is often realized through a pair of lasers, with the wavelength difference set to the target RF band, and the frequency of one laser scanned over the selected bandwidth. No wideband electronics are required in this scheme, and the large spectral operating range of the lasers essentially provides the output waveform with “unlimited” frequency and bandwidth. The down-conversion nature of the process also ensures the spectral purity of the generated waveform. However, as manipulating an optical frequency over a wide range has limited precision, the frequency accuracy of the generated waveform, which determines the linearity of the frequency modulation, is constrained [49], [68]. Moreover, linking the output frequency to other radar modules is challenging in complicated systems.

The choice of the O/E converter strongly depends on the output frequency. The operating frequency versus the bandwidth of the O/E converters is plotted in Fig. 5. The ellipses indicate only the typical performance of each category and do not suggest any performance restrictions.

At lower frequencies, PIN photodiodes (PDs) based on materials such as InGaAs have superior conversion efficiency, allowing the photodetection of signals up to  $\sim 50$  GHz with a maximum output power of +14 dBm [69]. The efficiency drastically decreases as the output frequency approaches the sub-THz region due to low-velocity hole transport [70].

This limitation can be addressed through a modified design known as the uni-traveling-carrier photodiode (UTC-PD), which

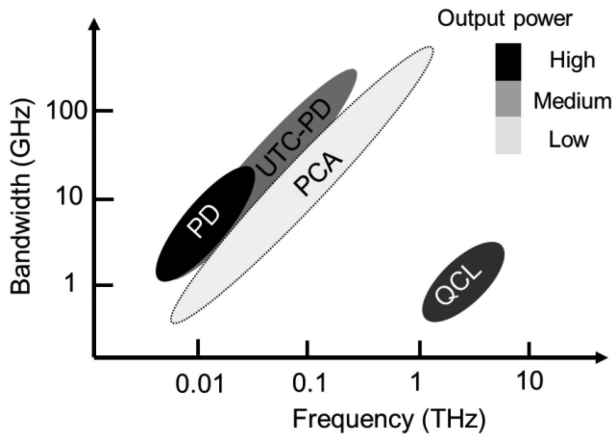


Fig. 5. Summary of the photonic radar components for radar waveform generation; the color intensity quantitatively indicates the output power of the devices. PD: photodiode; UTC-PD: uni-traveling-carrier photodiode; PCA: photoconductive antenna; QCL: quantum cascade lasers.

utilizes only electrons as active carriers. The output spectral range of the UTC-PD fills the “THz gap” between 0.1 and 1 THz, a region where the next generation of high-speed wireless communication devices is expected to be developed [52]. Currently, the UTC-PD is the most promising photomixer, with a wide bandwidth and a relatively high output power of  $\sim 1$  mW at the 300-GHz band [70]; however, this device is produced by only a few vendors due to its sophisticated manufacturing process.

In the THz region, the dominant photomixer is the photoconductive antenna (PCA), which is commercially available in many THz band imaging systems [30], [31], [32], [33]. It is mainly designed to receive ultrashort optical pulses produced by a femtosecond laser and transform these pulses into THz pulses in tens of picoseconds. Thus, this technique obtains superior spatial resolution for 3D imaging applications. The output power and sensitivity of the PCA are the lowest among the O/E converters described in this section; thus, a PCA is often paired with THz lenses for better focusing. As a result, PCA-based imaging systems are almost exclusively near-range imaging systems [31], [33].

In addition to these O/E conversion methods, semiconductor single-oscillator THz quantum cascade lasers (QCLs) [71], [72], [73], [74] have been investigated for imaging applications above the 1 THz band. QCLs have considerable integration potential and provide relatively high-power outputs on the order of milliwatts at frequencies above 1 THz. The operational requirement of a low temperature limits the practical application of QCLs; however, recent progress has been made in room-temperature imaging with a QCL device [72].

2) *Photonic Radar Receivers*: Unlike transmitters, which require the use of photonic devices, the receiver of a photonic radar can be either purely electronic or photonic. The operating frequencies of the electronic and photonic signal detection methods introduced below are plotted against the receiving bandwidth in Fig. 6. The color of each ellipse indicates the relative sensitivity. This plot only shows the expected performance of each category and suggests no performance restrictions.

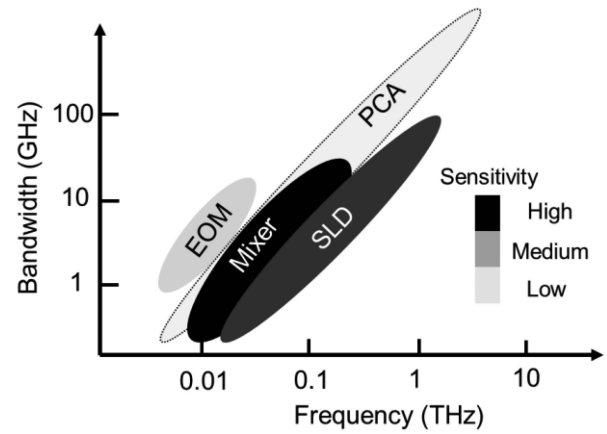


Fig. 6. Summary of the photonic radar components for coherent detection; the color intensity quantitatively indicates the sensitivity of the devices. EOM: electro-optical modulator; SLD: square-law detector; PCA: photoconductive antenna.

The fundamental mixers that are relatively mature and widely used in the microwave region can be applied in MMW radar systems to complete important frequency-modulated signal receiving processes. However, mixers above the MMW band are not typical due to fabrication difficulties and prohibitive costs [75].

Square-law detectors (SLDs) employing silicon complementary metal–oxide–semiconductor (CMOS) circuits, III-V high-electron-mobility transistors (HEMTs) [76], [77], Schottky barrier diodes (SBDs) [68], [78], and Fermi-level managed barrier diodes (FMBDs) [49], [79] are commonly used in the sub-THz band for signal mixing. In this case, the returned echo and the local copy of the transmitted waveform should be combined in a coupler before being sent to the detector [4], [48], [49]. This simplified configuration is equivalent to an unbalanced mixer, where both RF and LO signals remain in the IF output. However, although this poor signal isolation is undesirable in microwave radar and wireless communication systems, it has a relatively small effect on high-frequency, near-range imaging applications since the RF and LO signals are at much higher frequencies than the IF signals.

Integrating the abovementioned detectors with other components to produce compact receivers is still challenging due to the bandwidth limitations and propagation losses of conventional metal waveguides. Owing to the high directivity in high-frequency bands, spatial coupling using quasi-optical lenses and beam splitters is an alternative approach for retrieving the IF band radar signal [4], [48], [49]. This configuration addresses the bandwidth limitations and propagation losses; however, the bulky size and complicated optical alignment make it unsuitable for actual applications.

Recently, with the rapid development of THz band hardware boosted by 6G wireless communication, new materials have emerged for THz band waveguides. The THz band silicon waveguide platform is one candidate for integrating passive devices above the sub-THz band due to its superior low loss of  $<0.1$

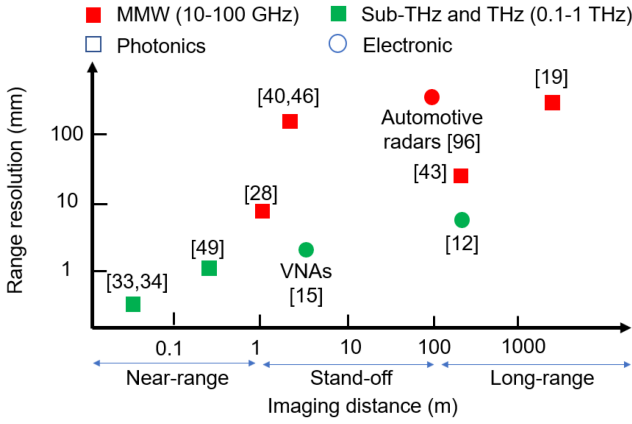


Fig. 7. Summary of the recent photonic radar imaging techniques in the MMW, sub-THz and THz bands. Some representative results using electronic systems are also included as references.

dB/cm [80], [81]. Integrated couplers at 0.6 and 1 THz have been installed for THz band imaging applications [4], [16].

Photonic reception of radar signals has recently become a popular research topic. Photonic mixing techniques based on electro-optical modulators (EOMs) have been introduced in many MMW band photonic radar systems. Mixing RF signals in the optical domain has been demonstrated to have several advantages over conventional electronic mixers, including ultrawide bandwidth, reduced phase noise, and compact size [19], [39], [82]. In addition, sub-THz and THz band photonic mixing has been achieved using PCAs. This is a relatively mature technique, and PCA pulse emitters have been widely used in THz pulse systems and THz band CW systems [33], [83]. Although these systems have large operating frequencies and wide bandwidths, the low sensitivity and small IF bandwidth are insufficient compared with electronic detectors in the sub-THz band, severely limiting the applicability of such systems.

### III. APPLICATIONS OF 3D PHOTONIC RADAR IMAGING SYSTEMS

The advantages of photonic radar systems are summarized in Section II. This Section introduces the imaging applications enabled by photonic radar systems. Specifically, the advantages of photonic systems are clarified using specific experiments and applications. The radar imaging techniques used in different approaches are summarized in Fig. 7, which corresponds to Table III. Generally, photonic radar systems in the MMW band are becoming mature technologies, and the imaging results of such systems are competitive and even outperform those of conventional electronic radar. The photonic radar system can become an alternative approach in this frequency band, which features reduced phase noise [19] or a compact system size [28].

Due to the limitations of photonic devices discussed in Section II, sub-THz band imaging techniques for electronic and photonic systems have only been applied in the laboratory. Although photonic radar systems have many advantages in this frequency band the laboratory systems' overall performance still needs to be improved to be compatible with high-end electronic

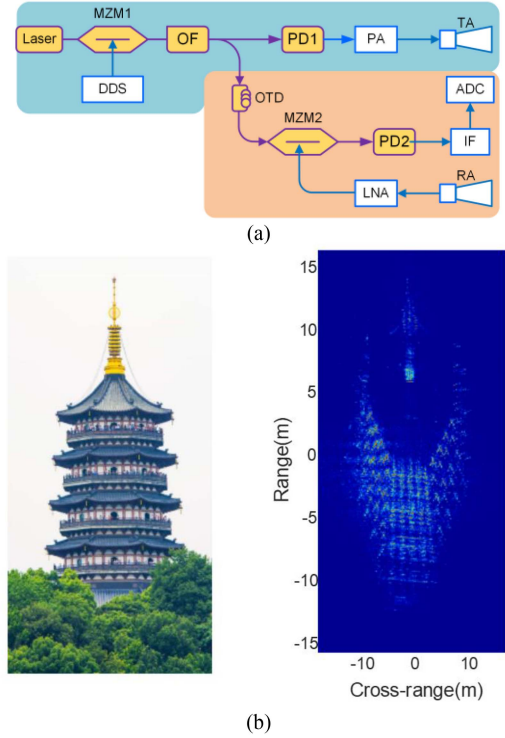


Fig. 8. SAR imaging using a photonic radar system operating in the Ka-band. (a) System configuration. MZM: Mach-Zehnder modulator; DDS: direct digital synthesizer; OF: optical filter; PD: photodetector; PA: power amplifier; TA: transmitting antenna; OTD: optical time delay; EDFA: erbium-doped fiber amplifier; LPF: low-pass filter; ADC: analog-to-digital converter; LNA: low-noise amplifier; RA: receiving antenna. (b) SAR imaging result of the Leifeng pagoda in Hangzhou, China. Reprinted with permission from [43].

systems, such as VNAs. The photonic systems at this frequency band are expected to become dominant with the rapid development of photonic devices. Meanwhile, the photonic systems become the immediate solutions for the near-range imaging application with above  $\sim 1$  THz with a sub-mm resolution.

#### A. MMW Photonic Radar Systems for Long-Range Imaging

Long-range imaging applications have been achieved almost exclusively below the 40-GHz band since key components, such as preamplifiers and mixers, are commercially available in this range. SAR imaging techniques are widely used in the MMW band, where no quasi-optical lenses that restrict the imaging range are needed.

As mentioned in Section II, high-spatial-resolution imaging is a primary aim of photonic radar systems. Using the SAR imaging technique, a Ka-band photonic radar system with a bandwidth of  $\sim 10$  GHz was demonstrated using the ROP scheme and a photonic mixer, as shown in Fig. 8 [43]. The radar waveform was modulated to the optical domain with an MZM, while another MZM operated as a photonic mixer at the receiving end. After precise numerical calibration, the 10.02 GHz bandwidth provided a range resolution of 1.68 cm. The cm-order range resolution obtained with the SAR algorithm provides information about detailed structures on the top of the Leifeng pagoda in Hangzhou, China. The moving radar platform was located a

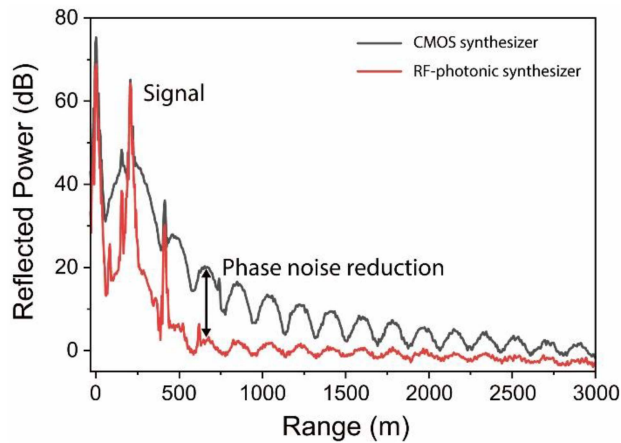


Fig. 9. Comparison of FMCW radar systems using photonic and electronic sources at 92 GHz. The systems measured back-reflection data from a building at a distance of  $\sim 207$  m using either the existing 92 GHz CMOS synthesizer of the radar or a photonic source. Phase noise fringes are significantly suppressed when using the low-noise photonics-based source. Reprinted with permission from [19].

distance of  $\sim 230$  m from the tower at an elevation angle of 13 degrees. Notably, although the imaging results are 2D images, the system can also be used for 3D imaging, as discussed in Section II-B.

The low phase noise is another advantage of photonic radar systems, as discussed in Section II-C. A recent MMW band photonic radar system operating at 94 GHz obtained better sensing results than a CMOS radar signal transmitter [19]. The proposed technique used a photonic source, which generated RF signals using a pair of distributed feedback lasers. Although the proposed system did not include a photonic mixer, the radar performance was considerably enhanced, as shown in Fig. 9. This finding highlights the potential of hybrid photonic radar systems with only photonic sources.

Mounting radar imaging systems on small platforms such as commercial drones can be advantageous in a variety of practical scenarios. In 2021, our group demonstrated an on-drone MMW radar system for inspecting pavement in a  $\sim 100$  m chimney [28]. The photonic radar system used the ROP scheme, with an optical fiber link between the radar module and the photonic source, as shown in Fig. 10. An ultrawide bandwidth of  $\sim 26$  GHz was achieved using an intensity modulator and the high-order sideband signal produced by the MMW synthesizer. The bulky RF signal source and modulators are connected to the  $\sim 900$ -g on-drone radar module using an optical fiber. The thickness of the pavement could be monitored in real time at an imaging distance of 1.4 m, as shown in Fig. 10(c). Compared with other on-drone radar imaging techniques enabled by electronic devices, this photonic radar system was demonstrated to be superior in terms of both the bandwidth and the weight of the radar module [28].

In addition to the wider bandwidth and lighter weight, frequency reconfigurability and band scalability can be obtained with photonic radar systems. Flexible waveform generation ranges from high frequencies to the Ka-band can be obtained with a cross-band bandwidth of up to 16 GHz, and multiband

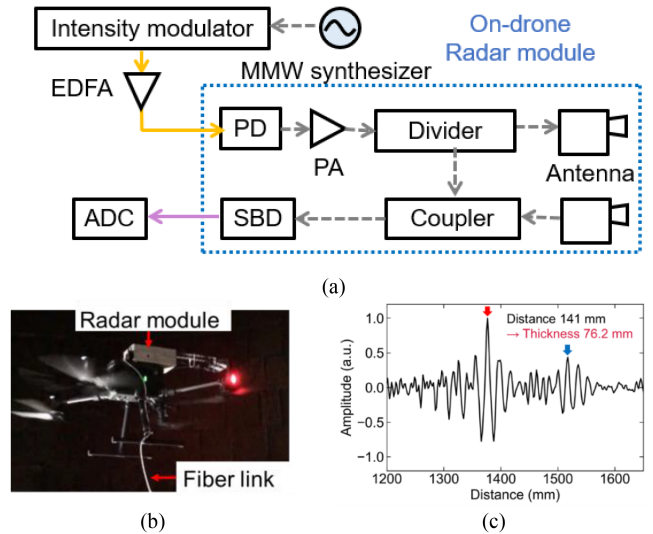


Fig. 10. Demonstration of an on-drone photonic radar system with an ultrawide bandwidth of 26 GHz. (a) System configuration. PD: photodetector; PA: power amplifier; EDFA: erbium-doped fiber amplifier; ADC: analog-to-digital converter. (b) Data acquisition inside the chimney. (c) Radar signal obtained at a height of  $\sim 3$  m; the thickness of the pavement can be monitored with the system.

system-level detection experiments have been carried out to verify the excellent ability of such systems [42].

### B. Sub-THz Radar Imaging at Standoff Distances

Some applications in this frequency band are security screening and quality control of production lines due to the mm-order resolution and standoff imaging distance [9], [65]. Both the 300 GHz and 600 GHz band security systems at standoff distances have been demonstrated with electronic radar systems and the quasi-optical beam focusing technique [20], [65]. However, due to the insufficient output power and limited focal depth using lenses, bandwidth information was mainly used to enhance the SNR rather than obtain 3D information.

Furthermore, these imaging distances are more challenging with photonic radar systems, which require a high-power source of at least mW-order and a preamplifier. Currently, some research groups, including ours, are developing photonic radar systems in this frequency band due to their large bandwidth and fast response times [4], [29], [48], [49], [50], [51].

As discussed in Section II, photonic sources using laser pairs are suitable for generating ultrawide bandwidths above 40 GHz. The large bandwidth in the optical domain enables large frequency sweeps in the THz domain. In [50], a laser system capable of doing a 200-GHz sweep within 30 ms was used to achieve a range resolution of  $\sim 0.5$  mm. Small thickness changes of  $\sim 50$   $\mu\text{m}$  in the coating materials of a metallic surface were detected and validated by comparing these changes with the results obtained by a commercial THz pulse system. However, due to the insufficient output power, this photonics-based 3D imaging system in the sub-THz band has only been applied in near-range applications using quasi-optical systems.

The above system was also investigated for SAR imaging applications with a minor output power of  $\sim 0.1$  mW in the 300-GHz band, as shown in Fig. 11(a) [49]. Due to the superior



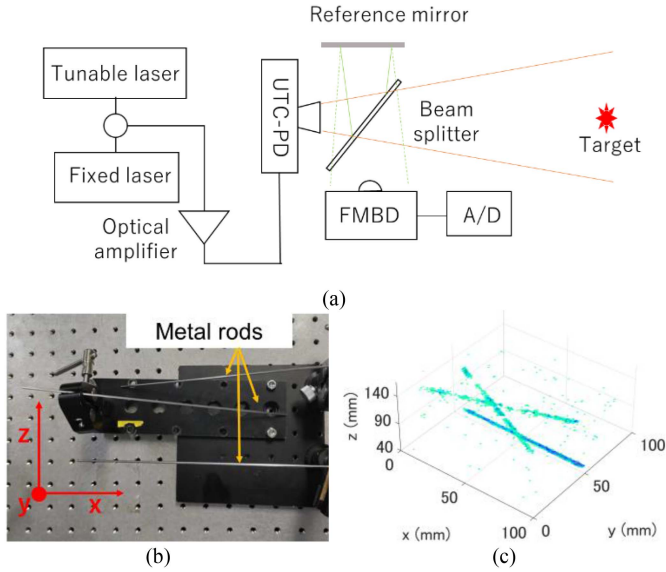


Fig. 11. 3D imaging using a photonic radar system in the 300-GHz band. (a) System configuration; (b) three distributed metal rods with 2 mm diameters as the imaging target; (c) SAR imaging result of the metal rods.

sensitivity of the THz detector [79] and the frequency-time calibration of the radar waveform, a metal plate at  $\sim 1$  m could be detected with a collimated beam with a range resolution of  $\sim 1$  mm. Furthermore, 3D images of distributed metal wires with 2 mm diameters were obtained with the SAR-based system, as shown in Fig. 11(b) and (c). Since the UTC-PD was integrated within the metallic waveguide, the present system can be combined with a recently commercialized preamplifier in the 300-GHz band. The presumable extended imaging range and the proven superior range resolution can potentially exceed those of the electronic radar system shown in Fig. 1, leading to many new possibilities and applications.

Considering the hardware limitations, the generation of a waveform with a very large frequency bandwidth above 100 GHz is another challenging task. The sweeping frequency speed and the linearity of the frequency sweep can both influence the radar imaging results. Advanced photonic waveform generation techniques are expected to be introduced in these frequency bands, and these approaches are discussed further in Section IV.

### C. Near-Range THz 3D Imaging Systems

The THz pulse imaging systems used for THz-TDS applications have the same energy limitations as the systems discussed in Section II. Short pulse signals with sufficient energy are more challenging to obtain than CW signals. Most existing THz pulse systems use quasi-optical lenses, and the imaging distance is usually less than the order of cm. In this case, precise inspection in the near range is a critical application.

Compared with MMW and sub-THz photonic imaging systems, THz pulse imaging systems have long been the dominant technology for near-range imaging since they can be uniquely achieved with photonic technologies. The THz pulse systems and THz-TDS technique were comprehensively reviewed in [5],

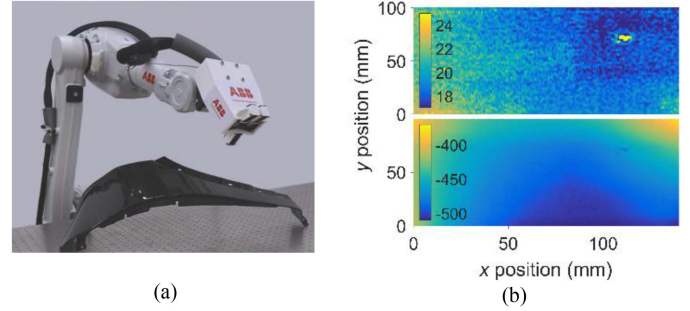


Fig. 12. (a) Photograph of a sensor mounted on an industrial robot beneath an automotive car part. (b) Upper: Surface thickness map (in  $\mu\text{m}$ ) of a primer-covered automotive paint sample measured by the sensor. A defect in the paint can be clearly identified in the upper right corner; Bottom: Measured distance (in  $\mu\text{m}$ ) between the sensor head and the car part after robot alignment, indicating the curvature of the sample. Reprinted with permission from [34].

showing numerous successful industrial applications, including defect inspection of polymers, woods, and card boxes, environmental sensing of gases, and inspections of coating materials, as discussed in [5], [9], [84].

Among these applications, the automotive industry is considered one of the biggest potential customers, and research related to this industry has attracted significant attention [34], [85], [86]. For example, the material properties of drying paints on automotive bodies were determined using a THz pulse system in [34]. The combination of a THz pulse system and robotic arms is an alternative approach for obtaining precise measurements at different positions. As shown in Fig. 12, a  $\sim 20$   $\mu\text{m}$  deep defect that was  $\sim 3$  mm in size was clearly detected by a 2D inspection system over a small region using the robotic arm platform. Another 3D imaging system using the THz pulse is demonstrated in [88], in which the 3D distribution of multilayered automotive paints was clearly distinguished using the THz pulse system.

The long acquisition time is another limitation of THz pulse systems. Recent works have attempted to replace the conventional mechanical delay stage with compact femtosecond fiber lasers [5], [17]. This replacement allows commercialized THz pulse systems to obtain fast sampling speeds of  $\sim 200$  Hz per pixel [87]. However, due to the dense spatial sampling in the THz band, 3D data acquisition is an expensive task. For example, the 3D data in the region of 80 by 300 mm were acquired over  $\sim 3$  hours [88]. The sensor array is still urgently needed to enhance the imaging speed for the near-range imaging applications.

Notably, an FMCW configuration with an ultrawide bandwidth of  $\sim 4$  THz enabled by PCAs has been reported, which obtains a superior range resolution of  $\sim 50$   $\mu\text{m}$  which is compatible with THz pulse techniques [33]. The purely photonic radar system has a simplified configuration, and PCAs are used as both the transmitter and receiver. Fig. 13 shows that the reflections from the upper and lower boundaries of the 42  $\mu\text{m}$  paint layer can be clearly distinguished. CW radar systems enabled by PCAs have great application potential due to their unlimited bandwidth, highly integrative design, and convenient interfaces with optical fibers. In addition, enhanced imaging speeds with THz pulse systems can be obtained due to the fast frequency

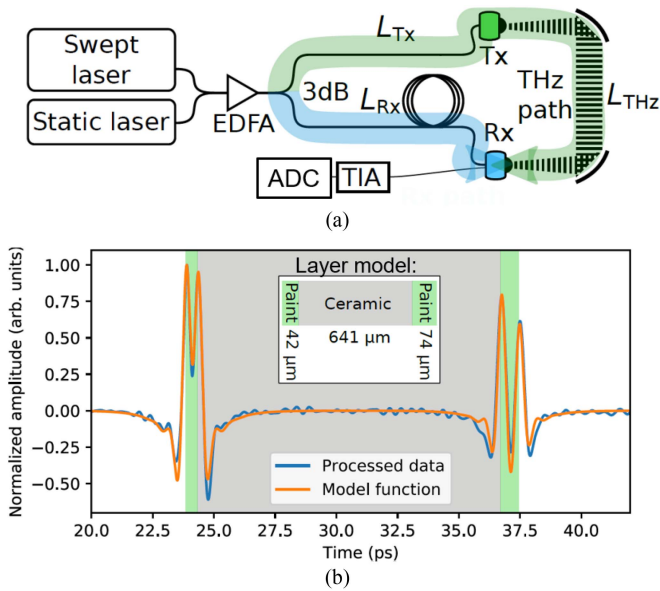


Fig. 13. FMCW radar system with a  $\sim 4$  THz bandwidth: (a) system configuration; Tx and Rx represent the PCAs. EDFA: erbium-doped fiber amplifier; TIA: Transimpedance amplifier; ADC: analog-to-digital converter. (b) 1D inspection results of a three-layer model. Reprinted with permission from [33].

sweeping speed of the laser. However, the lack of an interface with electronic devices, such as a preamplifier, is the primary limitation of this configuration.

## IV. DISCUSSIONS & FUTURE WORK

### A. Novel Photonic Radar Components

In future work, the performance of photonic THz 3D imaging systems can be readily enhanced by exploiting some recent progress in related research fields. For frequency-modulated optical carriers, in addition to the large bandwidth coverage and fast sweeping rate, which have been the primary focus of photonic approaches, high linearity, flat power roll-off and large SNR are the higher-order parameters that determine the spatial resolution. A novel optical carrier generator based on a recirculating optical frequency-shifting loop was developed to synthesize SFCWs with bandwidths of over 20 GHz and sweeping rates faster than  $1 \text{ GHz}/\mu\text{s}$  [89]. Moreover, as frequency sweeping is accumulated from a low-frequency microwave reference, the linearity reaches  $1e-7$ . The application of such optical carriers to photonic THz 3D imaging may remove the time-frequency calibration requirement mentioned in Section III-B, enabling the spatial resolution to reach the submillimeter regime.

In terms of frequency band scalability, there are a couple of candidates that may overcome the hurdles challenging the conventional approaches and provide high-quality optically carried THz tones. With the development of integrated photonic systems, micro-ring resonators with fundamental mode spacings ranging from tens of GHz to several THz offer an upgrade to the electro-optic combs with better power efficiency [90]. A low-noise multitone fiber laser based on stimulated Brillouin scattering [91], [92] has demonstrated high wavelength flexibility, high intercarrier coherence and extremely low frequency drift, supporting photonically generated THz carriers whose phase

noise does not scale with the output frequency. These results may inspire new photonic radar signal generation methods in addition to those discussed in Section II-C.

On the receiver side, progress with electro-optic mechanisms and materials has enabled optical fields modulated by RF signals ranging from the MMW to the lower THz range [93]. Analogous to the microwave counterpart [43], receiving THz signals in the optical domain may allow a variety of waveform manipulation methods based on photonic techniques to be applied, such as reconfigurable photonic filtering, ultrawideband photonic channelization and optical analog-to-digital conversion [35]. These novel methods may enable the transition of the photonic radar receivers summarized in Section II-C toward fully photonic and highly integrated systems.

### B. THz Band Integration and Array Systems

Integration and array techniques are the new trend in hardware technology for both photonic and electronic systems due to the small SWaP feature of the high-frequency components. They are also crucially important for realizing compact and lightweight imaging systems and achieving real-time imaging speeds, as discussed in Section II-B.

Significant research on integrated electronic radar transceivers in the THz band has been conducted with transistor devices such as heterostructure bipolar transistors (HBTs), HEMTs, and silicon CMOS transistors [94], [95], [96], [97]. However, breakthroughs are required to reduce costs and develop devices beyond the 200-GHz band.

Photonic technologies have also shown great potential for integration with array radar configurations [98]. Compact integrated photonic radar systems have already been developed, as demonstrated in [19], [38]. Photonic radar systems have many advantages, including their immunity to EM interference, multichannel signal manipulation using optical wavelength-division multiplexing (WDM) techniques, and ultrawideband phase shifting. These are unique features that can only be achieved with photonic technologies. However, the existing array radar systems operate below the MMW band, where many advantages of photonic radar systems cannot be fully demonstrated. For example, optical fibers are lossless and easy to set up for array systems, but electronic switches and multiple PD devices using expensive and lossy coaxial cables or metal waveguides are still needed.

Another exciting technique is the high-power photonic source enabled with the UTC-PD array [99], [100]. As mentioned in Section III-B, the existing photonic sources in the sub-THz bands suffer from insufficient output power. Moreover, combining these sources with electronic amplifiers limits the bandwidth in this frequency band. The UTC-PD array, which aims to achieve mW-order output power by combining multiple UTC-PDs [99], is expected to be the ultimate approach for enhancing both wireless communication and radar imaging applications with improved output power and beam-steering ability [100].

To address these limitations, electronic and photonic devices have been efficiently integrated, demonstrating the advantages of both technologies [101]. We believe that the array technique represents the future trend of THz imaging.

### C. Future Applications

The radar imaging technique is one of the most important tools for remote sensing applications, as higher imaging resolution is always necessary to meet different application demands [2], [9]. Photonic radar systems in the MMW band have been rapidly developed in recent years, and many photonic radar systems have been used in remote sensing applications instead of conventional electronic radar devices, as discussed in Section III.

Sub-THz band photonic radar systems with large bandwidths of more than 100 GHz, which offer millimeter-order resolution, have great potential as next-generation remote sensing tools, which was validated by laboratory experiments [12], [15], [49]. However, due to the low output power, the existing photonic radar imaging systems in the sub-THz band need to be improved. Integrated systems with electronic and photonic devices may be an alternative method for improving sub-THz band photonic radar techniques [101]. For example, photonic devices with electronic interfaces, such as UTC-PDs, allow photomixers to be combined with electronic preamplifiers, although the bandwidth may be limited [70], [102].

In comparison, a powerful photonic source, such as the UTC-PDs array introduced in Section IV-B, is still urgently needed to demonstrate the true potential of photonic devices. Furthermore, long-range imaging applications can be realized due to the superior resolution of sub-THz band photonic radar systems. Despite security and production line inspection applications, automotive radar systems can be further improved using sub-THz technologies [103]. Furthermore, as noted by researchers in the remote sensing field, THz band remote sensing techniques may inspire new applications and scientific questions in research fields such as agriculture [104], ice cloud monitoring, and space exploration [105].

Another interesting research direction is the evolution of wireless technologies toward 6G and beyond. New research fields, such as integrated communication and sensing (ICS), have been extensively investigated. Many studies have examined photonic THz wireless communication systems with hundreds of Gbit/s and even Tbit/s data rates in various atmospheric windows [53]. Sharing almost identical system architectures, data transmission processes and 3D imaging schemes across different millimeter and/or THz bands may be possible with single photonic platforms that obtain both fast communication speeds and higher imaging resolution [59].

### V. CONCLUSION

This article briefly reviewed the existing photonic radar techniques for imaging up to the THz band. The advantages of photonic radar systems in the MMW band were discussed. Photonic radar systems are the only method enabling near-range imaging with ultra-high resolution in the order of  $\mu\text{m}$ . In comparison, high-resolution imaging applications in the sub-THz band remain at the laboratory stage, enabled by photonic techniques and high-end electronic instruments. These frequency bands will be explored extensively in future works with the development of wireless communication toward 6G and beyond. Many new technologies and applications using photonic techniques have

been proposed in recent works, as discussed in Section IV. This progress suggests that 3D imaging systems enabled by photonic technologies will soon move out of the laboratory toward real-world industrial applications.

### REFERENCES

- [1] N. Metje et al., "Mapping the underworld - State-of-the-Art review," *Tunnelling Underground Space Technol.*, vol. 22, no. 5–6, pp. 568–586, 2007, doi: [10.1016/j.tust.2007.04.002](https://doi.org/10.1016/j.tust.2007.04.002).
- [2] D. M. Mittleman, "Twenty years of terahertz imaging," *Opt. Exp.*, vol. 26, no. 8, pp. 9417–9431, 2018, doi: [10.1364/oe.26.009417](https://doi.org/10.1364/oe.26.009417).
- [3] A. Batra et al., "Short-range SAR imaging from GHz to THz waves," *IEEE J. Microw.*, vol. 1, no. 2, pp. 574–585, Apr. 2021, doi: [10.1109/jmw.2021.3063343](https://doi.org/10.1109/jmw.2021.3063343).
- [4] L. Yi et al., "Towards practical terahertz imaging system with compact continuous wave transceiver," *J. Lightw. Technol.*, vol. 39, no. 24, pp. 7850–7861, Dec. 2021, doi: [10.1109/JLT.2021.3092779](https://doi.org/10.1109/JLT.2021.3092779).
- [5] J. Neu and C. A. Schmuttenmaer, "Tutorial: An introduction to terahertz time domain spectroscopy (THz-TDS)," *J. Appl. Phys.*, vol. 124, no. 23, 2018, Art. no. 231101, doi: [10.1063/1.5047659](https://doi.org/10.1063/1.5047659).
- [6] P. Mehrotra, B. Chatterjee, and S. Sen, "EM-wave biosensors: A review of RF, microwave, mm-wave and optical sensing," *Sensors (Switzerland)*, vol. 19, no. 5, 2019, Art. no. 1013, doi: [10.3390/s19051013](https://doi.org/10.3390/s19051013).
- [7] G. Valušis, A. Lisauskas, H. Yuan, W. Knap, and H. G. Roskos, "Roadmap of terahertz imaging 2021," *Sensors*, vol. 21, no. 12, 2021, Art. no. 4092, doi: [10.3390/s21124092](https://doi.org/10.3390/s21124092).
- [8] Y. H. Tao, A. J. Fitzgerald, and V. P. Wallace, "Non-contact, non-destructive testing in various industrial sectors with terahertz technology," *Sensors*, vol. 20, no. 3, Jan. 2020, Art. no. 712, doi: [10.3390/s20030712](https://doi.org/10.3390/s20030712).
- [9] D. Nübler and J. Jonuscheit, "Terahertz based non-destructive testing (NDT)," *tm-Technisches Messen*, vol. 88, no. 4, 2021, pp. 199–210, doi: [10.1515/teme-2019-0100](https://doi.org/10.1515/teme-2019-0100).
- [10] Z. Wang, T. Chang, and H. L. Cui, "Review of active millimeter wave imaging techniques for personnel security screening," *IEEE Access*, vol. 7, pp. 148336–148350, 2019, doi: [10.1109/ACCESS.2019.2946736](https://doi.org/10.1109/ACCESS.2019.2946736).
- [11] K. Asaka, Y. Hirano, K. Tatsumi, K. Kasahara, and T. Tajime, "A pseudo-random frequency modulation continuous wave coherent lidar using an optical field correlation detection method," *Opt. Rev.*, vol. 5, no. 5, pp. 310–314, 1998, doi: [10.1007/s10043-998-0310-7](https://doi.org/10.1007/s10043-998-0310-7).
- [12] M. Caris et al., "300 GHz radar for high resolution SAR and ISAR applications," in *Proc. 16th Int. Radar Symp.*, 2015, pp. 577–580, doi: [10.1109/IRS.2015.7226313](https://doi.org/10.1109/IRS.2015.7226313).
- [13] H. Matsumoto, I. Watanabe, A. Kasamatsu, and Y. Monnai, "Integrated terahertz radar based on leaky-wave coherence tomography," *Nature Electron.*, vol. 3, no. 2, pp. 122–129, 2020, doi: [10.1038/s41928-019-0357-4](https://doi.org/10.1038/s41928-019-0357-4).
- [14] H. Momiyama et al., "Improvement of the depth resolution of swept-source THz-OCT for non-destructive inspection," *Opt. Exp.*, vol. 28, no. 8, pp. 12279–12293, 2020, doi: [10.1364/oe.386680](https://doi.org/10.1364/oe.386680).
- [15] D. Damyanov et al., "High-resolution long-range THz imaging for tunable continuous-wave systems," *IEEE Access*, vol. 8, pp. 151997–152007, 2020, doi: [10.1109/ACCESS.2020.3017821](https://doi.org/10.1109/ACCESS.2020.3017821).
- [16] R. Koala et al., "Ultra-low-loss and broadband all-silicon dielectric waveguides for WR-1 band (0.75–1.1 THz) modules," *Photonics*, vol. 9, no. 8, Jul. 2022, Art. no. 515, doi: [10.3390/photonics9080515](https://doi.org/10.3390/photonics9080515).
- [17] H. I. G. Uerboukha and K. A. N. Allappan, "Toward real-time terahertz imaging," *Adv. Opt. Photon.*, vol. 10, no. 4, pp. 843–938, 2018.
- [18] K. Siddiq, M. K. Hobden, S. R. Pennock, and R. J. Watson, "Phase noise in FMCW radar systems," *IEEE Trans. Aerosp. Electron. Syst.*, vol. 55, no. 1, pp. 70–81, Feb. 2019, doi: [10.1109/TAES.2018.2847999](https://doi.org/10.1109/TAES.2018.2847999).
- [19] E. A. Kittlaus et al., "A low-noise photonic heterodyne synthesizer and its application to millimeter-wave radar," *Nature Commun.*, vol. 12, no. 1, 2021, Art. no. 4397, doi: [10.1038/s41467-021-24637-0](https://doi.org/10.1038/s41467-021-24637-0).
- [20] A. V. Shchepetilnikov et al., "New ultra-fast sub-terahertz linear scanner for postal security screening," *J. Infrared, Millimeter, Terahertz Waves*, vol. 41, pp. 655–664, 2020, doi: [10.1007/s10762-020-00692-4](https://doi.org/10.1007/s10762-020-00692-4).
- [21] S.-P. Han et al., "InGaAs Schottky barrier diode array detector for a real-time compact terahertz line scanner," *Opt. Exp.*, vol. 21, no. 22, pp. 25874–25882, 2013, doi: [10.1364/oe.21.025874](https://doi.org/10.1364/oe.21.025874).
- [22] Q. Song, Y. Zhao, A. Redo-Sanchez, C. Zhang, and X. Liu, "Fast continuous terahertz wave imaging system for security," *Opt. Commun.*, vol. 282, no. 10, pp. 2019–2022, 2009, doi: [10.1016/j.optcom.2009.02.019](https://doi.org/10.1016/j.optcom.2009.02.019).

- [23] T. Miyamoto, A. Yamaguchi, and T. Mukai, "Terahertz imaging system with resonant tunneling diodes," *Japanese J. Appl. Phys.*, vol. 55, no. 3, 2016, Art. no. 032201, doi: [10.7567/JJAP.55.032201](https://doi.org/10.7567/JJAP.55.032201).
- [24] L. Yi et al., "Imaging applications with a single resonant tunneling diode transceiver in 300-GHz band," in *Proc. Int. Topical Meet. Microw. Photon.*, 2020, pp. 120–123, doi: [10.23919/MWP48676.2020.9314482](https://doi.org/10.23919/MWP48676.2020.9314482).
- [25] H. Konno, A. Dobroui, S. Suzuki, M. Asada, and H. Ito, "Discrete fourier transform radar in the terahertz-wave range based on a resonant-tunneling-diode oscillator," *Sensors*, vol. 21, no. 13, 2021, Art. no. 4367, doi: [10.3390/s21134367](https://doi.org/10.3390/s21134367).
- [26] T. Maekawa, H. Kanaya, S. Suzuki, and M. Asada, "Oscillation up to 1.92 THz in resonant tunneling diode by reduced conduction loss," *Appl. Phys. Exp.*, vol. 9, no. 2, 2016, Art. no. 024101, doi: [10.7567/APEX.9.024101](https://doi.org/10.7567/APEX.9.024101).
- [27] T. Hiraoka et al., "Injection locking and noise reduction of resonant tunneling diode terahertz oscillator," *APL Photon.*, vol. 6, no. 2, 2021, Art. no. 021301, doi: [10.1063/5.0033459](https://doi.org/10.1063/5.0033459).
- [28] H. Tokunaga, Y. Tamenori, L. Yi, and T. Nagatsuma, "Drone-mounted optical fiber-fed millimeter-wave radar," in *Proc. IEEE 46th Int. Conf. Infrared, Millimeter Terahertz Waves*, 2021, pp. 1/2, doi: [10.1109/IRMMW-THz50926.2021.9567059](https://doi.org/10.1109/IRMMW-THz50926.2021.9567059).
- [29] A. Kanno, N. Sekine, Y. Uzawa, I. Hosako, and T. Kawanishi, "300-GHz FM-CW radar system by optical frequency comb generation," in *Proc. Eur. Microw. Conf.*, 2015, pp. 558–561, doi: [10.1109/EuMC.2015.7345824](https://doi.org/10.1109/EuMC.2015.7345824).
- [30] S. Hisatake et al., "Phase-sensitive terahertz self-heterodyne system based on photodiode and low-temperature-grown GaAs photoconductor at 1.55 nm," *IEEE Sensors J.*, vol. 13, no. 1, pp. 31–36, Jan. 2012, doi: [10.1109/jsen.2012.2218281](https://doi.org/10.1109/jsen.2012.2218281).
- [31] S. Busch et al., "Terahertz transceiver concept," *Opt. Exp.*, vol. 22, no. 14, pp. 16841–16846, 2014, doi: [10.1364/oe.22.016841](https://doi.org/10.1364/oe.22.016841).
- [32] D. R. Bacon, J. Madéo, and K. M. Dani, "Photoconductive emitters for pulsed terahertz generation," *J. Opt. (United Kingdom)*, vol. 23, no. 6, 2021, Art. no. 064001, doi: [10.1088/2040-8986/abf6ba](https://doi.org/10.1088/2040-8986/abf6ba).
- [33] L. Liebermeister et al., "Optoelectronic frequency-modulated continuous-wave terahertz spectroscopy with 4 THz bandwidth," *Nature Commun.*, vol. 12, no. 1, Dec. 2021, Art. no. 1071, doi: [10.1038/s41467-021-21260-x](https://doi.org/10.1038/s41467-021-21260-x).
- [34] J. L. M. V. Mechelen, A. Frank, and D. J. H. C. Maas, "Thickness sensor for drying paints using THz spectroscopy," *Opt. Exp.*, vol. 29, no. 5, pp. 7514–7525, 2021, doi: [10.1364/oe.418809](https://doi.org/10.1364/oe.418809).
- [35] P. Ghelfi et al., "A fully photonics-based coherent radar system," *Nature*, vol. 507, no. 7492, pp. 341–345, 2014, doi: [10.1038/nature13078](https://doi.org/10.1038/nature13078).
- [36] X. Zhang et al., "Novel RF-source-free reconfigurable microwave photonic radar," *Opt. Exp.*, vol. 28, no. 9, pp. 13650–13661, 2020, doi: [10.1364/oe.386285](https://doi.org/10.1364/oe.386285).
- [37] J. Qin, Q. Zhou, W. Xie, Y. Dong, and W. Hu, "Linearization of broadband frequency sweep for temperature tuned DFB laser using an optoelectronic feedback loop," in *Proc. Asia Commun. Photon. Conf.*, 2015, pp. 3–5, doi: [10.1364/acpc.2015.asu3i.3](https://doi.org/10.1364/acpc.2015.asu3i.3).
- [38] S. Li et al., "Chip-based microwave-photonic radar for high-resolution imaging," *Laser Photon. Rev.*, vol. 14, no. 10, 2020, Art. no. 1900239, doi: [10.1002/lpor.201900239](https://doi.org/10.1002/lpor.201900239).
- [39] Z. Tang, Y. Li, J. Yao, and S. Pan, "Photonics-based microwave frequency mixing: Methodology and applications," *Laser Photon. Rev.*, vol. 14, no. 1, 2020, Art. no. 1800350, doi: [10.1002/lpor.201800350](https://doi.org/10.1002/lpor.201800350).
- [40] Y. Yao et al., "Demonstration of ultra-high-resolution photonics-based K-band inverse synthetic aperture radar imaging," in *Proc. IEEE Opt. Fiber Commun. Conf. Expo.*, 2018, pp. 1–3.
- [41] F. Zhang et al., "Photonics-based broadband radar for high-resolution and real-time inverse synthetic aperture imaging," *Opt. Exp.*, vol. 25, no. 14, pp. 16274–16281, 2017, doi: [10.1364/oe.25.016274](https://doi.org/10.1364/oe.25.016274).
- [42] A. Wang et al., "Microwave photonic radar system with ultra-flexible frequency-domain tunability," *Opt. Exp.*, vol. 29, no. 9, pp. 13887–13898, 2021, doi: [10.1364/oe.423952](https://doi.org/10.1364/oe.423952).
- [43] A. Wang et al., "Ka-band microwave photonic ultra-wideband imaging radar for capturing quantitative target information," *Opt. Exp.*, vol. 26, no. 16, pp. 20708–20717, 2018, doi: [10.1364/oe.26.020708](https://doi.org/10.1364/oe.26.020708).
- [44] C. Ma et al., "Microwave photonic imaging radar with a sub-centimeter-level resolution," *J. Light. Technol.*, vol. 38, no. 18, pp. 4948–4954, Sep. 2020, doi: [10.1109/JLT.2020.3000488](https://doi.org/10.1109/JLT.2020.3000488).
- [45] S. Pan and Y. Zhang, "Microwave photonic radars," *J. Light. Technol.*, vol. 38, no. 19, pp. 5450–5484, Oct. 2020, doi: [10.1109/JLT.2020.2993166](https://doi.org/10.1109/JLT.2020.2993166).
- [46] Y. Liu, Z. Zhang, M. Burla, and B. J. Eggleton, "11-GHz-bandwidth photonic radar using MHz electronics," *Laser Photon. Rev.*, vol. 16, no. 4, 2022, Art. no. 2100549, doi: [10.1002/lpor.202100549](https://doi.org/10.1002/lpor.202100549).
- [47] A. Rashidinejad et al., "Photonic generation and wireless transmission of W-band arbitrary waveforms with high time-bandwidth products," in *Proc. Conf. Lasers Electro-Optics - Laser Sci. Photon. Appl.*, 2014, pp. 1–2, doi: [10.1364/cleo\\_si.2014.sm1g.1](https://doi.org/10.1364/cleo_si.2014.sm1g.1).
- [48] T. Isogawa et al., "Tomographic imaging using photonically generated low-coherence terahertz noise sources," *IEEE Trans. Terahertz Sci. Technol.*, vol. 2, no. 5, pp. 485–492, Sep. 2012, doi: [10.1109/TTHZ.2012.2208745](https://doi.org/10.1109/TTHZ.2012.2208745).
- [49] L. Yi et al., "Ultra-Wideband frequency modulated continuous wave photonic radar system for three-dimensional terahertz synthetic aperture radar imaging," *J. Light. Technol.*, vol. 40, no. 20, pp. 6719–6728, Oct. 2022, doi: [10.1109/JLT.2022.3193397](https://doi.org/10.1109/JLT.2022.3193397).
- [50] R. Kaname, L. Yi, and T. Nagatsuma, "Investigation on 600-GHz-Band FMCW photonic radar system for a flexible inspection distance," in *Proc. IEEE Asia-Pacific Microw. Conf.*, 2021, pp. 437–439, doi: [10.1109/APMC52720.2021.9661657](https://doi.org/10.1109/APMC52720.2021.9661657).
- [51] S. Wang et al., "A terahertz photonic imaging radar system based on inverse synthetic aperture technique," in *Proc. Opto-Electron. Commun. Conf.*, 2021, pp. 6–8, doi: [10.1364/oec.2021.m3e.4](https://doi.org/10.1364/oec.2021.m3e.4).
- [52] T. Nagatsuma et al., "Terahertz wireless communications based on photonics technologies," *Opt. Exp.*, vol. 21, no. 20, pp. 23736–23747, 2013, doi: [10.1364/oe.21.023736](https://doi.org/10.1364/oe.21.023736).
- [53] T. Nagatsuma, G. Ducourmau, and C. C. Renaud, "Advances in terahertz communications accelerated by photonics," *Nature Photon.*, vol. 10, no. 6, pp. 371–379, 2016, doi: [10.1038/nphoton.2016.65](https://doi.org/10.1038/nphoton.2016.65).
- [54] J. V. D. Kruk, C. P. A. Wapenaar, J. T. Fokkema, and P. M. V. D. Berg, "Three-dimensional imaging of multicomponent ground-penetrating radar data," *Geophysics*, vol. 68, no. 4, pp. 1241–1254, 2003, doi: [10.1190/1.1598116](https://doi.org/10.1190/1.1598116).
- [55] D. Oloumi, "Ultra-wideband synthetic aperture radar imaging: Theory and applications," M.S. thesis, Dept. Electr. Comput. Eng., Univ. Alberta, Edmonton, AB, Canada, Sep. 2016.
- [56] T. Tseng et al., "High-depth-resolution 3-dimensional radar-imaging system based on a few-cycle W-band photonic millimeter-wave pulse generator," *Opt. Exp.*, vol. 21, no. 12, pp. 10416–10423, 2013, doi: [10.1364/OE.21.014109](https://doi.org/10.1364/OE.21.014109).
- [57] T. Nagatsuma, T. Ikeo, and H. Nishii, "Terahertz imaging based on optical coherence tomography," *Photon. Res.*, vol. 2, no. 4, pp. 64–69, 2014, doi: [10.1109/ICECom.2013.6684745](https://doi.org/10.1109/ICECom.2013.6684745).
- [58] S. Mazahir, S. Ahmed, and M.-S. Alouini, "A survey on joint communication-radar systems," *Front. Commun. Netw.*, vol. 1, no. Feb., 2021, Art. no. 619483, doi: [10.3389/frcmn.2020.619483](https://doi.org/10.3389/frcmn.2020.619483).
- [59] M. Lei et al., "Photonics-aided integrated sensing and communications in mmW bands based on a DC-offset QPSK-encoded LFMCW," *Opt. Exp.*, vol. 30, no. 24, pp. 43088–43103, 2022, doi: [10.1364/oe.474055](https://doi.org/10.1364/oe.474055).
- [60] C. Özdemir, Ş. Demirci, E. Yiğit, and B. Yılmaz, "A review on migration methods in B-scan ground penetrating radar imaging," *Math. Problems Eng.*, vol. 2014, 2014, Art. no. 280738, doi: [10.1155/2014/280738](https://doi.org/10.1155/2014/280738).
- [61] A. Moreira et al., "A tutorial on synthetic aperture radar," *IEEE Geosci. Remote Sens. Mag.*, vol. 1, no. 1, pp. 6–43, Mar. 2013, doi: [10.1109/MGRS.2013.2248301](https://doi.org/10.1109/MGRS.2013.2248301).
- [62] C. Cafforio, C. Prati, and F. Rocca, "SAR data focusing using seismic migration techniques," *IEEE Trans. Aerosp. Electron. Syst.*, vol. 27, no. 2, pp. 194–207, Mar. 1991, doi: [10.1109/7.78293](https://doi.org/10.1109/7.78293).
- [63] M. Kim, E. S. Lee, D. W. Park, I. M. Lee, and K. H. Park, "Hexagonal polygon mirror based terahertz imaging system by using telecentric f- $\theta$  lens," in *Proc. Int. Conf. Infrared, Millimeter, Terahertz Waves*, 2019, pp. 1–2, doi: [10.1109/IRMMW-THz.2019.8873863](https://doi.org/10.1109/IRMMW-THz.2019.8873863).
- [64] R. Kaname, T. Sagisaka, L. Yi, and T. Nagatsuma, "600-GHz-Band terahertz imaging system using frequency-independent concave mirror," in *Proc. Int. Topical Meeting Microw. Photon.*, 2020, pp. 58–61, doi: [10.23919/MWP48676.2020.9314504](https://doi.org/10.23919/MWP48676.2020.9314504).
- [65] K. B. Cooper et al., "Fast high-resolution terahertz radar imaging at 25 meters," *Proc. SPIE*, vol. 7671, 2010, Art. no. 76710Y, doi: [10.1117/12.850395](https://doi.org/10.1117/12.850395).
- [66] A. I. Hernandez-Serrano and E. Pickwell-MacPherson, "Low cost and long-focal-depth metallic axicon for terahertz frequencies based on parallel-plate-waveguides," *Sci. Rep.*, vol. 11, no. 1, 2021, Art. no. 3005, doi: [10.1038/s41598-021-82503-x](https://doi.org/10.1038/s41598-021-82503-x).
- [67] Y. Wang, L. Yi, M. Tonouchi, and T. Nagatsuma, "High-speed 600 GHz-band terahertz imaging scanner system with enhanced focal depth," *Photonics*, vol. 9, no. 12, Nov. 2022, Art. no. 913, doi: [10.3390/photonic9120913](https://doi.org/10.3390/photonic9120913).
- [68] Z. Yang et al., "Robust photonic terahertz vector imaging scheme using an optical frequency comb," *J. Light. Technol.*, vol. 40, no. 9, pp. 2717–2723, May 2022, doi: [10.1109/JLT.2022.3146438](https://doi.org/10.1109/JLT.2022.3146438).

- [69] Y. Yi, T. Umezawa, A. Kanno, and T. Kawanishi, "50 GHz high photocurrent PIN-PD and its thermal effect," in *Proc. 27th Optoelectron. Commun. Conf. Int. Conf. Photon. Switching Comput.*, 2022, pp. 01–03, doi: [10.23919/OECC/PSC53152.2022.9849985](https://doi.org/10.23919/OECC/PSC53152.2022.9849985).
- [70] T. Ishibashi, Y. Muramoto, T. Yoshimatsu, and H. Ito, "Unitraveling-carrier photodiodes for terahertz applications," *IEEE J. Sel. Topics Quantum Electron.*, vol. 20, no. 6, Nov./Dec. 2014, Art. no. 3804210, doi: [10.1109/JSTQE.2014.2336537](https://doi.org/10.1109/JSTQE.2014.2336537).
- [71] T. J. Smith et al., "A hybrid THz imaging system with a 100-Pixel CMOS imager and a 3.25–3.50 THz quantum cascade laser frequency comb," *IEEE Solid-State Circuits Lett.*, vol. 2, no. 9, pp. 151–154, Sep. 2019, doi: [10.1109/LSSC.2019.2933332](https://doi.org/10.1109/LSSC.2019.2933332).
- [72] A. Nakanishi, K. Fujita, K. Horita, and H. Takahashi, "Terahertz imaging with room-temperature terahertz difference-frequency quantum-cascade laser sources," *Opt. Exp.*, vol. 27, no. 3, pp. 1884–1893, 2019, doi: [10.1364/oe.27.001884](https://doi.org/10.1364/oe.27.001884).
- [73] P. Dean et al., "Terahertz imaging using quantum cascade lasers - A review of systems and applications," *J. Phys. D: Appl. Phys.*, vol. 47, no. 37, 2014, Art. no. 374008, doi: [10.1088/0022-3727/47/37/374008](https://doi.org/10.1088/0022-3727/47/37/374008).
- [74] A. A. Danylov et al., "Terahertz inverse synthetic aperture radar (ISAR) imaging with a quantum cascade laser transmitter," *Opt. Exp.*, vol. 18, no. 15, pp. 16264–16272, 2010, doi: [10.1364/oe.18.016264](https://doi.org/10.1364/oe.18.016264).
- [75] S. Wang et al., "Dual-band THz photonic pulses enabling synthetic mm-scale range resolution," *IEEE Photon. Technol. Lett.*, vol. 30, no. 20, pp. 1760–1763, Oct. 2018, doi: [10.1109/LPT.2018.2868774](https://doi.org/10.1109/LPT.2018.2868774).
- [76] E. N. Grossman, K. Leong, X. Mei, and W. Deal, "Low-frequency noise and passive imaging with 670 GHz HEMT low-noise amplifiers," *IEEE Trans. Terahertz Sci. Technol.*, vol. 4, no. 6, pp. 749–752, Nov. 2014, doi: [10.1109/TTHZ.2014.2352035](https://doi.org/10.1109/TTHZ.2014.2352035).
- [77] D. Cibiraitė et al., "TeraFET multi-pixel THz array for a confocal imaging system," in *Proc. IEEE 44th Int. Conf. Infrared, Millimeter, Terahertz Waves*, 2019, pp. 1–2, doi: [10.1109/IRMMW-THz.2019.8874217](https://doi.org/10.1109/IRMMW-THz.2019.8874217).
- [78] S. Dülme et al., "Ultra-low phase-noise photonic terahertz imaging system based on two-tone square-law detection," *Opt. Exp.*, vol. 28, no. 20, pp. 29631–29643, 2020, doi: [10.1364/oe.400405](https://doi.org/10.1364/oe.400405).
- [79] H. Ito and T. Ishibashi, "InP/InGaAs fermi-level managed barrier diode for broadband and low-noise terahertz-wave detection," *Japanese J. Appl. Phys.*, vol. 56, no. 1, 2017, Art. no. 014101, doi: [10.7567/JJAP.56.014101](https://doi.org/10.7567/JJAP.56.014101).
- [80] K. Tsuruda, M. Fujita, and T. Nagatsuma, "Extremely low-loss terahertz waveguide based on silicon photonic-crystal slab," *Opt. Exp.*, vol. 23, no. 25, pp. 31977–31990, 2015, doi: [10.1364/oe.23.031977](https://doi.org/10.1364/oe.23.031977).
- [81] R. A. S. D. Koala, M. Fujita, and T. Nagatsuma, "Nanophotonics-inspired all-silicon waveguide platforms for terahertz integrated systems," *Nanophotonics*, vol. 11, no. 9, pp. 1741–1759, 2022, doi: [10.1515/nanoph-2021-0673](https://doi.org/10.1515/nanoph-2021-0673).
- [82] S. Pinna et al., "Photonics-based radar for sub-mm displacement sensing," *IEEE J. Sel. Topics Quantum Electron.*, vol. 23, no. 2, pp. 168–175, Mar./Apr. 2017, doi: [10.1109/JSTQE.2016.2635800](https://doi.org/10.1109/JSTQE.2016.2635800).
- [83] S. Hisatake, J. Y. Kim, K. Ajito, and T. Nagatsuma, "Self-heterodyne spectrometer using uni-traveling-carrier photodiodes for terahertz-wave generators and optoelectronic mixers," *J. Light. Technol.*, vol. 32, no. 20, pp. 3683–3689, Oct. 2014, doi: [10.1109/JLT.2014.2321004](https://doi.org/10.1109/JLT.2014.2321004).
- [84] M. Naftaly, N. Vieweg, and A. Deninger, "Industrial applications of terahertz sensing: State of play," *Sensors (Switzerland)*, vol. 19, no. 19, 2019, Art. no. 4203, doi: [10.3390/s19194203](https://doi.org/10.3390/s19194203).
- [85] K. Su, Y. C. Shen, and J. A. Zeitler, "Terahertz sensor for non-contact thickness and quality measurement of automobile paints of varying complexity," *IEEE Trans. Terahertz Sci. Technol.*, vol. 4, no. 4, pp. 432–439, Jul. 2014, doi: [10.1109/TTHZ.2014.2325393](https://doi.org/10.1109/TTHZ.2014.2325393).
- [86] F. Ellrich et al., "Terahertz quality inspection for automotive and aviation industries," *J. Infrared, Millimeter, Terahertz Waves*, vol. 41, no. 4, pp. 470–489, 2020, doi: [10.1007/s10762-019-00639-4](https://doi.org/10.1007/s10762-019-00639-4).
- [87] J. H. Yim et al., "Rapid 3D-imaging of semiconductor chips using THz time-of-flight technique," *Appl. Sci.*, vol. 11, no. 11, 2021, Art. no. 4770, doi: [10.3390/app11114770](https://doi.org/10.3390/app11114770).
- [88] S. Krimi et al., "Highly accurate thickness measurement of multi-layered automotive paints using terahertz technology," *Appl. Phys. Lett.*, vol. 109, no. 2, 2016, Art. no. 021105, doi: [10.1063/1.4955407](https://doi.org/10.1063/1.4955407).
- [89] Y. Lv and Z. Zheng, "Photonic generation of highly-linear ultra-wideband stepped-frequency microwave signals with up to 610<sup>6</sup> time-bandwidth product," *J. Light. Technol.*, vol. 40, no. 4, pp. 1036–1042, Feb. 2022, doi: [10.1109/jlt.2021.3127949](https://doi.org/10.1109/jlt.2021.3127949).
- [90] M. Tan et al., "Photonic RF arbitrary waveform generator based on a soliton crystal micro-comb source," *J. Light. Technol.*, vol. 38, no. 22, pp. 6221–6226, Nov. 2020, doi: [10.1109/JLT.2020.3009655](https://doi.org/10.1109/JLT.2020.3009655).
- [91] T. Tetsumoto et al., "Optically referenced 300 GHz millimetre-wave oscillator," *Nature Photon.*, vol. 15, no. 7, pp. 516–522, 2021, doi: [10.1038/s41566-021-00790-2](https://doi.org/10.1038/s41566-021-00790-2).
- [92] L. Yi et al., "300-GHz-band wireless communication using a low phase noise photonic source," *Int. J. Microw. Wirel. Technol.*, vol. 12, no. 7, pp. 551–558, 2020, doi: [10.1017/S175907872000029X](https://doi.org/10.1017/S175907872000029X).
- [93] M. Burla et al., "500 GHz plasmonic Mach-Zehnder modulator enabling sub-THz microwave photonics," *APL Photon.*, vol. 4, no. 5, 2019, Art. no. 056106, doi: [10.1063/1.5086868](https://doi.org/10.1063/1.5086868).
- [94] K. S. Choi, D. R. Utomo, and S. G. Lee, "A fully integrated 490-GHz CMOS heterodyne imager adopting second subharmonic resistive mixer structure," *IEEE Microw. Wirel. Compon. Lett.*, vol. 29, no. 10, pp. 673–676, Oct. 2019, doi: [10.1109/LMWC.2019.2936685](https://doi.org/10.1109/LMWC.2019.2936685).
- [95] D. Čibiraitė-Lukenskiene et al., "Passive detection and imaging of human body radiation using an uncooled field-effect transistor-based THz detector," *Sensors (Switzerland)*, vol. 20, no. 15, 2020, Art. no. 4087, doi: [10.3390/s20154087](https://doi.org/10.3390/s20154087).
- [96] P. Hillger, J. Grzyb, R. Jain, and U. R. Pfeiffer, "Terahertz imaging and sensing applications with silicon-based technologies," *IEEE Trans. Terahertz Sci. Technol.*, vol. 9, no. 1, pp. 1–19, Jan. 2019, doi: [10.1109/TTHZ.2018.2884852](https://doi.org/10.1109/TTHZ.2018.2884852).
- [97] P. Hillger et al., "A 128-pixel system-on-a-chip for real-time super-resolution terahertz near-field imaging," *IEEE J. Solid-State Circuits*, vol. 53, no. 12, pp. 3599–3612, Dec. 2018, doi: [10.1109/JSSC.2018.2878817](https://doi.org/10.1109/JSSC.2018.2878817).
- [98] S. Pan, X. Ye, Y. Zhang, and F. Zhang, "Microwave photonic array radars," *IEEE J. Microw.*, vol. 1, no. 1, pp. 176–190, Jan. 2021, doi: [10.1109/jmw.2020.3034583](https://doi.org/10.1109/jmw.2020.3034583).
- [99] K. Kondo, Y. Matsuo, and K. Kato, "60-times power enhancement of 300-GHz terahertz wave by 8-arrayed UTC-PDs," in *Proc. IEEE 26th Microoptics Conf.*, 2021, pp. 1–2, doi: [10.23919/MOC52031.2021.9598087](https://doi.org/10.23919/MOC52031.2021.9598087).
- [100] M. Che, Y. Matsuo, K. Kondo, and K. Kato, "Arrayed uni-traveling-carrier photodiodes for pulsed THz wave beam steering," in *Proc. Int. Topical Meet. Microw. Photon.*, 2021, pp. 1–4, doi: [10.1109/MWP53341.2021.9639421](https://doi.org/10.1109/MWP53341.2021.9639421).
- [101] K. Sengupta, T. Nagatsuma, and D. M. Mittleman, "Terahertz integrated electronic and hybrid electronic-Photonic systems," *Nature Electron.*, vol. 1, no. 12, pp. 622–635, 2018, doi: [10.1038/s41928-018-0173-2](https://doi.org/10.1038/s41928-018-0173-2).
- [102] A. Tessmann et al., "A 600 GHz low-noise amplifier module," in *Proc. IEEE MTT-S Int. Microw. Symp. Dig.*, 2014, pp. 1–3, doi: [10.1109/MWSYM.2014.6848456](https://doi.org/10.1109/MWSYM.2014.6848456).
- [103] F. Norouzian, E. G. Hoare, E. Marchetti, M. Cherniakov, and M. Gashinova, "Next generation, low-THz automotive radar-the potential for frequencies above 100 GHz," in *Proc. Int. Radar Symp.*, 2019, pp. 1–7, doi: [10.23919/IRS.2019.8767461](https://doi.org/10.23919/IRS.2019.8767461).
- [104] L. Afsah-Hejri et al., "Terahertz spectroscopy and imaging: A review on agricultural applications," *Comput. Electron. Agriculture*, vol. 177, 2020, Art. no. 105628, doi: [10.1016/j.compag.2020.105628](https://doi.org/10.1016/j.compag.2020.105628).
- [105] M. Nakagawa et al., "Compact 480-GHz radiometer calibration unit with specular reflection absorber for atmospheric remote sensor on-board microsatellite," *IEEE Trans. Terahertz Sci. Technol.*, vol. 11, no. 5, pp. 486–494, Sep. 2021, doi: [10.1109/TTHZ.2021.3095436](https://doi.org/10.1109/TTHZ.2021.3095436).

**Li Yi** (Member, IEEE) received the B.Sc. degree in geophysics from the School of Ocean and Earth Science, Tongji University, Shanghai, China, in 2011, and the M.E. and Ph.D. degrees in environmental studies from the Graduate School of Environmental Studies, Tohoku University, Sendai, Japan, in 2014 and 2017, respectively. He was a Researcher of the National Institute of Advanced Industrial Science and Technology till 2018. He is currently an Assistant Professor with the Graduate School of Engineering Science, Osaka University, Osaka, Japan. His research interests include photonics-based millimeter/terahertz waves devices and applications, which include sensing/imaging techniques, wireless communication and signal processing techniques. He is a Member of the Institute of Electronics, Information and Communication Engineers, Japan.

Dr. Yi was the recipient of the Student Paper Competition Prize of URSI Japan Radio Science Meeting in 2015, President Award of environmental study of Tohoku University in 2017, and Young Scientists Award of IEICE, SANE, in 2018. He is a Member of the Institute of Electronics, Information and Communication Engineers, Japan, and is currently an Associate Editor for the *IEICE Electronics Express*.

**Yihan Li** (Member, IEEE) received the B.S. degree in physics from the University of Science and Technology of China, Hefei, China, and the Ph.D. degree in electrical engineering from Purdue University, West Lafayette, IN, USA. From 2015 to 2018, he was a Laser Research Scientist with the Boulder Research Lab of IMRA America, Longmont, CO, USA, where he had worked on the development and applications of fiber optical frequency comb. Since 2018, he has been an Associate Professor with the School of Electronics and Information Engineering, and later with the School of Integrated Circuit Science and Technology, Beihang University, Beijing, China. His research interests include microwave photonics, ultrafast optics, optical frequency comb, ultra-wideband signal generation and processing, and photonic THz communications. Dr. Li is a Member of the Committee of Laser and Terahertz in Space of the Chinese Society of Astronautics and a Member of Optica (the Optical Society of America).

**Tadao Nagatsuma** (Fellow, IEEE) received the B.S., M.S., and Ph.D. degrees in electronic engineering from Kyushu University, Fukuoka, Japan, in 1981, 1983, and 1986, respectively. In 1986, he joined Electrical Communications Laboratories, Nippon Telegraph and Telephone Corporation (NTT), Atsugi, Japan. From 1999 to 2002, he was a Distinguished Technical Member with NTT Telecommunications Energy Laboratories. From 2003 to 2007, he was a Group Leader with NTT Microsystem Integration Laboratories and was an NTT Research Professor from 2007 to 2009. Since 2007, he has been with Osaka University, Osaka, Japan, where he is currently a Professor with the Division of Advanced Electronics and Optical Science, Department of Systems Innovation, Graduate School of Engineering Science. His research interests include ultrafast electronics and millimeter-wave and terahertz photonics.

Dr. Nagatsuma is a Fellow of the Institute of Electronics, Information and Communication Engineers (IEICE), Japan, and a Fellow of the Electromagnetics Academy. He is currently an Associate Editor for IEEE TRANSACTIONS TERAHERTZ SCIENCE AND TECHNOLOGY, and a President of the Terahertz Systems Consortium and a Past-Vice President of the IEICE. He was the recipient of numerous awards, including the 1989 IEICE Young Engineers Award, 1992 IEEE Andrew R. Chi Best Paper Award, 1997 Okochi Memorial Award, 1998 Japan Microwave Prize, 2000 Ministers Award of the Science and Technology Agency, 2002 and 2011 Asia-Pacific Microwave Conference Prize, 2004 YRP (Yokosuka Research Park) Award, 2006 Asia-Pacific Microwave Photonics Conference Award, 2006 European Microwave Conference Prize, 2007 Achievement Award presented by the IEICE, 2008 Maejima Award, 2011 Recognition from Kinki Bureau of Telecommunications, Ministry of Internal Affairs and Communications, 2011 Commendation for Science and Technology by the Ministry of Education, Culture, Sports, Science and Technology, 2014 IEEE Tatsuo Ito Award, and 2020 Distinguished Achievement and Contributions Award by the IEICE.